

## ELECTRONIC SUPPLEMETARY INFORMATION

### Reversible transformation between Cu(I)-thiophenolate coordination polymers displaying luminescence and electrical properties

Javier Troyano,<sup>a</sup> Óscar Castillo,<sup>b</sup> Pilar Amo-Ochoa,<sup>a,c</sup> J. Ignacio Martínez,<sup>d</sup> Félix Zamora,<sup>\*,a,c,e</sup> and Salomé Delgado<sup>\*, a,c</sup>

---

<sup>a</sup> Departamento de Química Inorgánica, Universidad Autónoma de Madrid, 28049 Madrid, Spain.

<sup>b</sup> Departamento de Química Inorgánica, Universidad del País Vasco, UPV/EHU, Apartado 644, E-48080 Bilbao, Spain.

<sup>c</sup> Institute for Advanced Research in Chemical Sciences (IAdChem) Universidad Autónoma de Madrid, 28049 Madrid, Spain.

<sup>d</sup> Departamento de Nanoestructuras, Superficies, Recubrimientos y Astrofísica Molecular, Instituto de Ciencia de Materiales de Madrid (ICMM-CSIC), 28049 Madrid, Spain.

<sup>e</sup> Instituto Madrileño de Estudios Avanzados en Nanociencia (IMDEA Nanociencia), Cantoblanco, 28049 Madrid, Spain.

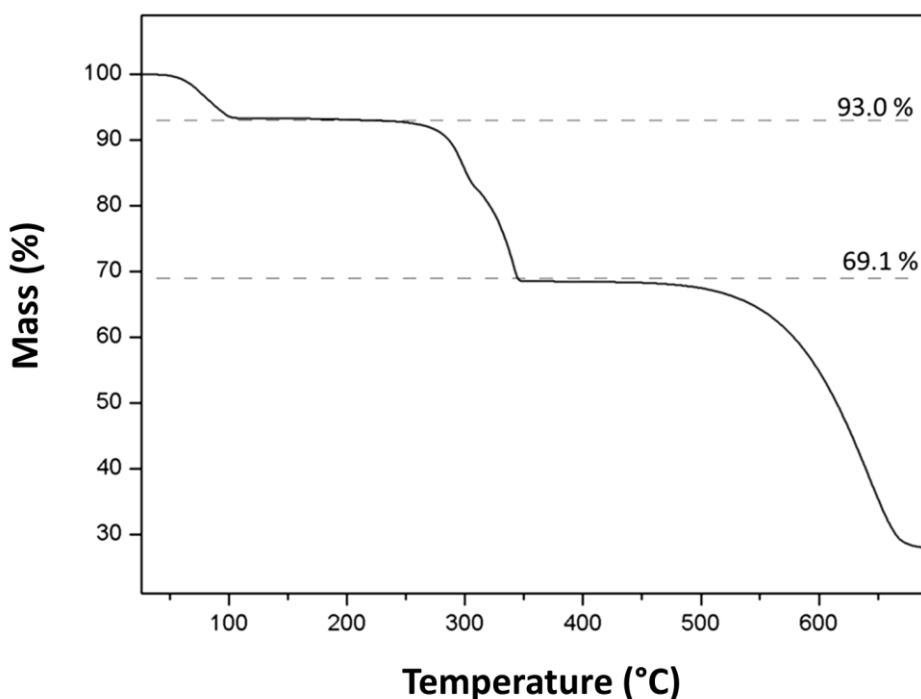


**Fig. S1.** TGA curve of **1** under  $\text{N}_2$  atmosphere at a heating rate of  $5\text{ }^{\circ}\text{C min}^{-1}$ . The dashed lines indicate the expected weight changes for the proposed transformations.

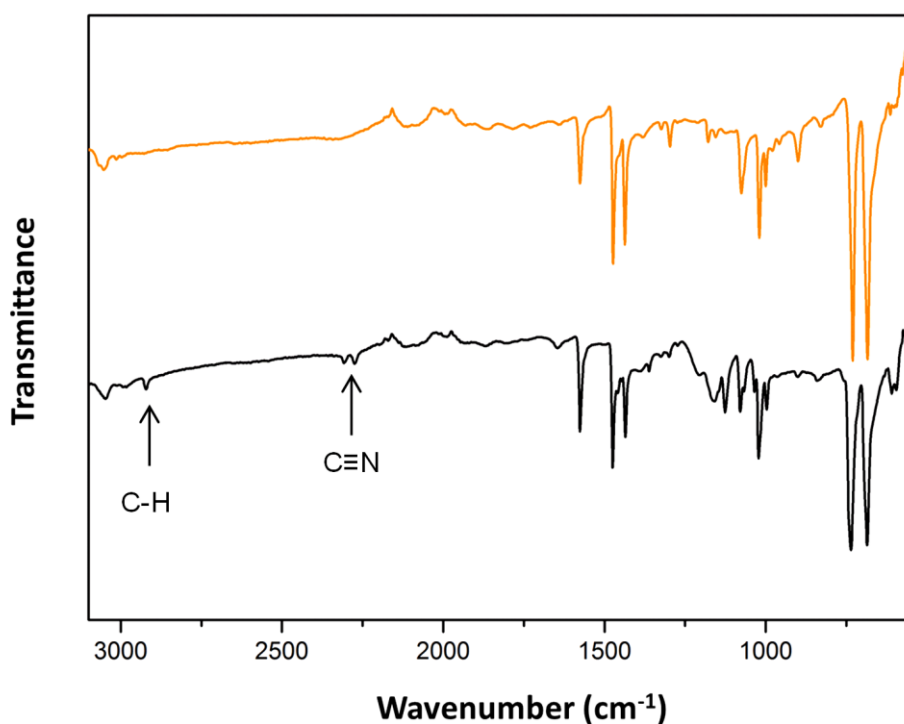


**Fig. S2.** FT-IR spectra of polycrystalline solid sample of **1** before heating (black) and after heating at  $140\text{ }^{\circ}\text{C}$  under argon atmosphere for 30 min (orange) in KBr pellets.

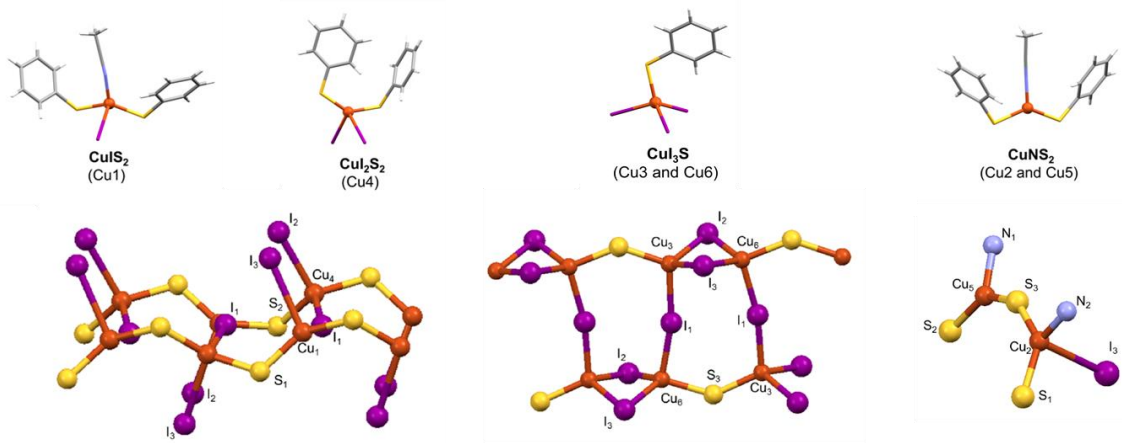


**Fig. S3.** Coordination environments around the different copper(I) atoms in **1**.

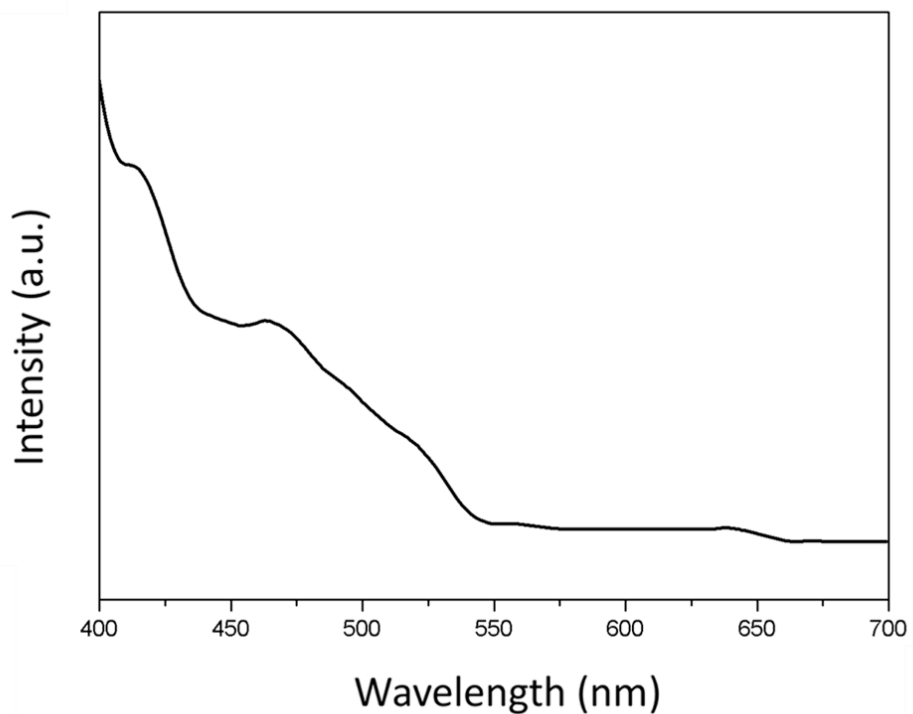


**Fig. S4.** Emission spectra of thiophenol (TP) upon excitation at 359 nm at room temperature.

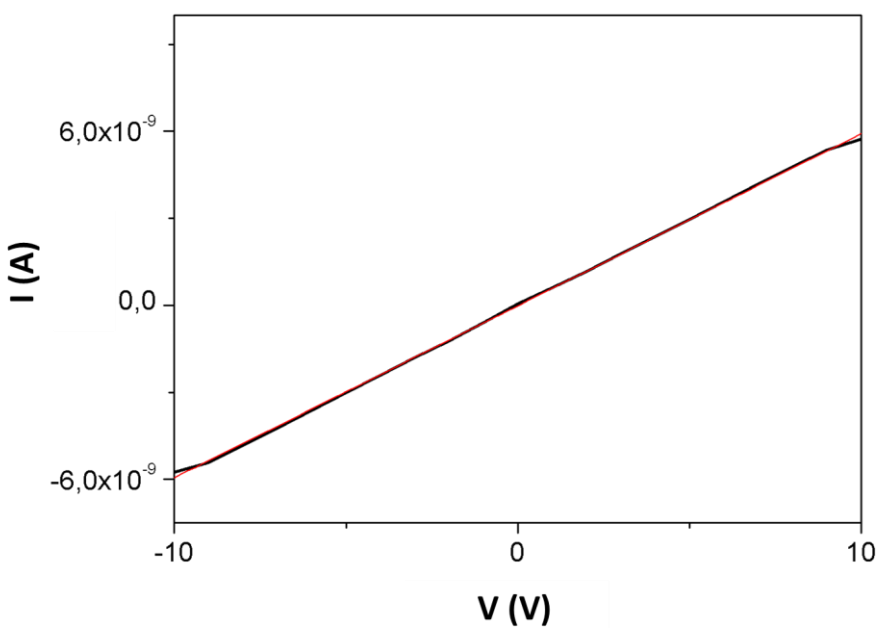


**Fig. S5.** Intensity (A) versus voltage (V) (black) and linear fit (red) corresponding to one pressed pellet of compound **1**, measured with the two-contact method, with graphite paint at 300 K.

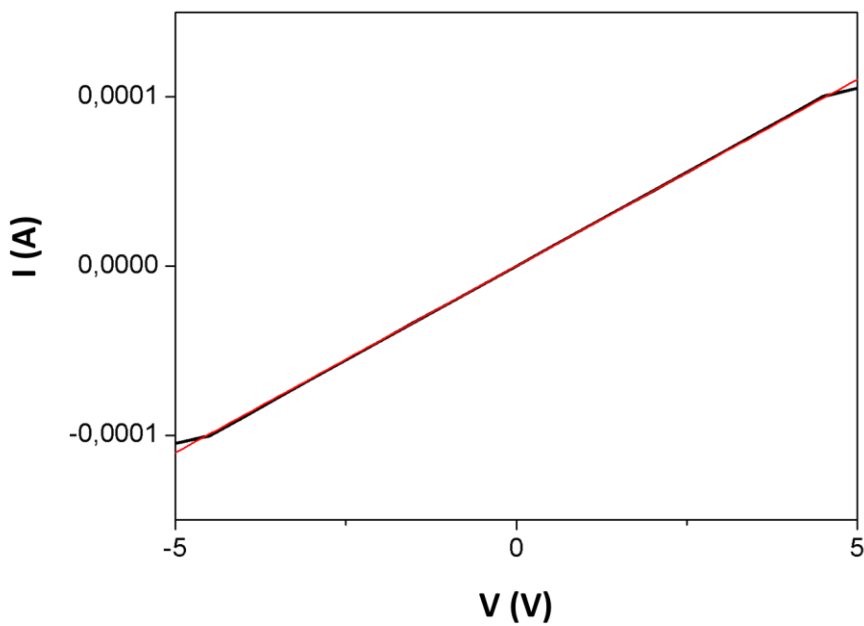


**Fig. S6.** Intensity (A) versus voltage (V) and linear fit (red) corresponding to one pressed pellet of compound **2**, measured with the two-contact method, with graphite paint at 300 K.

**Table S1.** Copper environment distances ( $\text{\AA}$ ) in **1**

<b>Cu1—S1</b>	2.258(2)
<b>Cu1—S1<sup>i</sup></b>	2.240(2)
<b>Cu1—I1</b>	2.6491(14)
<b>Cu2—N2</b>	1.977(9)
<b>Cu2—S1</b>	2.230(2)
<b>Cu2—S3<sup>ii</sup></b>	2.279(3)
<b>Cu3—S3<sup>ii</sup></b>	2.334(3)
<b>Cu3—I1</b>	2.6903(15)
<b>Cu3—I2<sup>i</sup></b>	2.7066(16)
<b>Cu3—I3<sup>i</sup></b>	2.7343(16)
<b>Cu4—S2</b>	2.262(3)
<b>Cu4—S2<sup>ii</sup></b>	2.282(2)
<b>Cu4—I1</b>	2.6869(14)
<b>Cu4—I2<sup>i</sup></b>	2.9062(16)
<b>Cu5—N1</b>	1.986(9)
<b>Cu5—S2</b>	2.223(3)
<b>Cu5—S3</b>	2.269(3)
<b>Cu6—S3</b>	2.354(3)
<b>Cu6—I1</b>	2.6494(14)
<b>Cu6—I2</b>	2.6729(16)
<b>Cu6—I3</b>	2.6635(16)
<b>Cu2…Cu3</b>	2.883(2)
<b>Cu3…Cu5<sup>ii</sup></b>	2.934(2)
Symmetry codes: (i) $x, 3/2-y, -1/2+z$ ; (ii) $x, 3/2-y, 1/2+z$ .	

**Table S2.** Copper environment angles ( $^{\circ}$ ) in **1**

<b>S1—Cu1—S1<sup>i</sup></b>	139.46(12)
<b>S1—Cu1—I1</b>	99.45(7)
<b>S1<sup>i</sup>—Cu1—I1</b>	108.48(8)
<b>N2—Cu2—S1</b>	118.1(3)
<b>N2—Cu2—S3<sup>ii</sup></b>	105.8(3)
<b>S1—Cu2—S3<sup>ii</sup></b>	132.79(10)
<b>S3<sup>ii</sup>—Cu3—I1</b>	111.56(7)
<b>S3<sup>ii</sup>—Cu3—I2<sup>i</sup></b>	120.20(8)
<b>S3<sup>ii</sup>—Cu3—I3<sup>i</sup></b>	114.34(8)
<b>I1—Cu3—I2<sup>i</sup></b>	103.65(5)
<b>I1—Cu3—I3<sup>i</sup></b>	103.22(5)
<b>I2<sup>i</sup>—Cu3—I3<sup>i</sup></b>	101.96(5)
<b>S2—Cu4—S2<sup>ii</sup></b>	133.30(11)
<b>S2—Cu4—I1</b>	106.20(8)
<b>S2—Cu4—I2<sup>i</sup></b>	109.25(8)
<b>S2<sup>ii</sup>—Cu4—I1</b>	98.00(7)
<b>S2<sup>ii</sup>—Cu4—I2<sup>ii</sup></b>	105.71(7)
<b>I1—Cu4—I2<sup>ii</sup></b>	98.60(5)
<b>N1—Cu5—S2</b>	116.8(3)
<b>N1—Cu5—S3</b>	106.9(3)
<b>S2—Cu5—S3</b>	136.31(10)
<b>S3—Cu6—I1</b>	97.82(7)
<b>S3—Cu6—I2</b>	117.17(8)
<b>S3—Cu6—I3</b>	119.88(8)
<b>I1—Cu6—I2</b>	106.39(5)
<b>I1—Cu6—I3</b>	109.82(5)
<b>I2—Cu6—I3</b>	104.77(5)

Symmetry codes: (i)  $x$ ,  $3/2-y$ ,  $-1/2+z$ ; (ii)  $x$ ,  $3/2-y$ ,  $1/2+z$ .

**Table S3.** Copper environment distances ( $\text{\AA}$ ) in **2**

<b>Cu1—S1</b>	2.2982(19)
<b>Cu1—S1<sup>i</sup></b>	2.2697(16)
<b>Cu1—S1<sup>ii</sup></b>	2.3033(16)

Symmetry codes: (i) 1/2-y,x,-1/2-z; (ii) 1/2-y,x,1/2-z.

**Table S4.** Copper environment angles ( $^{\circ}$ ) in **2**

<b>S1—Cu1—S1<sup>i</sup></b>	112.87(4)
<b>S1—Cu1—S1<sup>ii</sup></b>	133.47(5)
<b>S1<sup>i</sup>—Cu1—S1<sup>ii</sup></b>	113.61(7)
<b>Cu1—S1—Cu1<sup>iii</sup></b>	97.61(9)
<b>Cu1—S1—Cu1<sup>iv</sup></b>	79.95(8)
<b>Cu1<sup>iii</sup>—S1—Cu1<sup>iv</sup></b>	113.61(6)

Symmetry codes: (i) 1/2-y,x,-1/2-z; (ii) 1/2-y,x,1/2-z; (iii) y,1/2-x,-1/2-z; (iv) y,1/2-x,1/2-z.

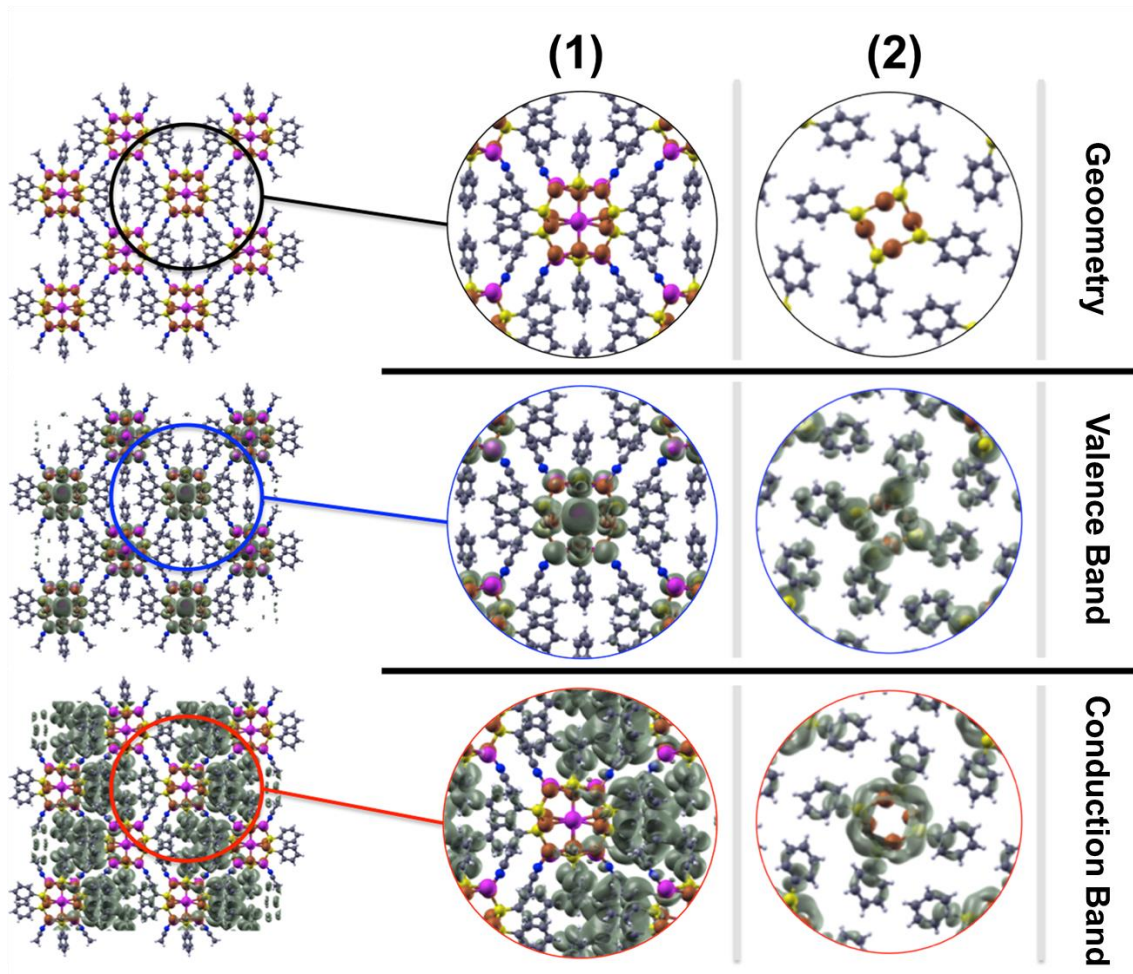


**Fig. S7.** Computed valence (middle panels) and conduction (bottom panels) band orbital electron isodensities ( $10^{-4} \text{ e}^- \text{\AA}^{-3}$ ) for the compounds **1** and **2**. Clean geometries are also shown for a better visualization (top panels).

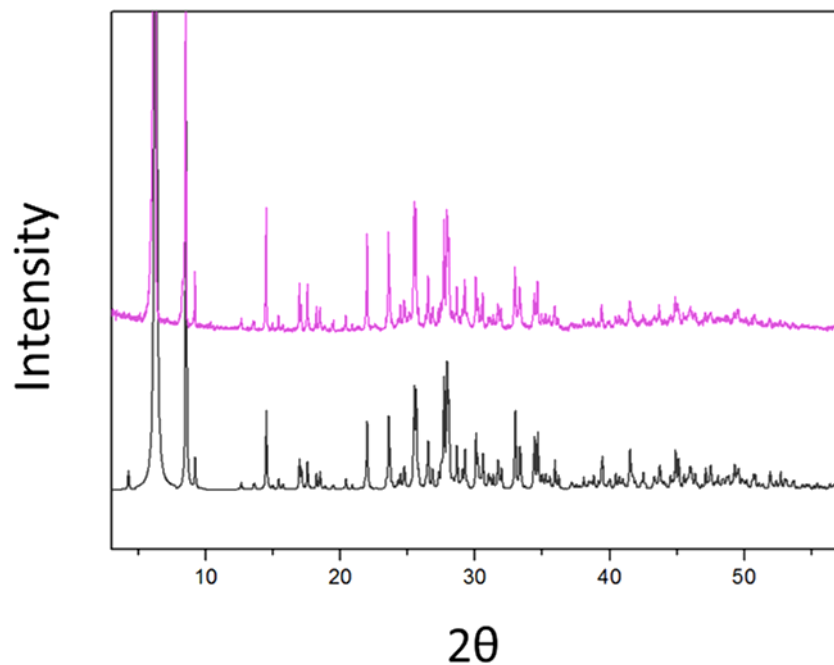


**Fig. S8.** Experimental (purple) and simulated (black) XRPD patterns of  $[\text{Cu}_6\text{I}_3(\text{TP})_3(\text{MeCN})_2]_n$  (**1**).

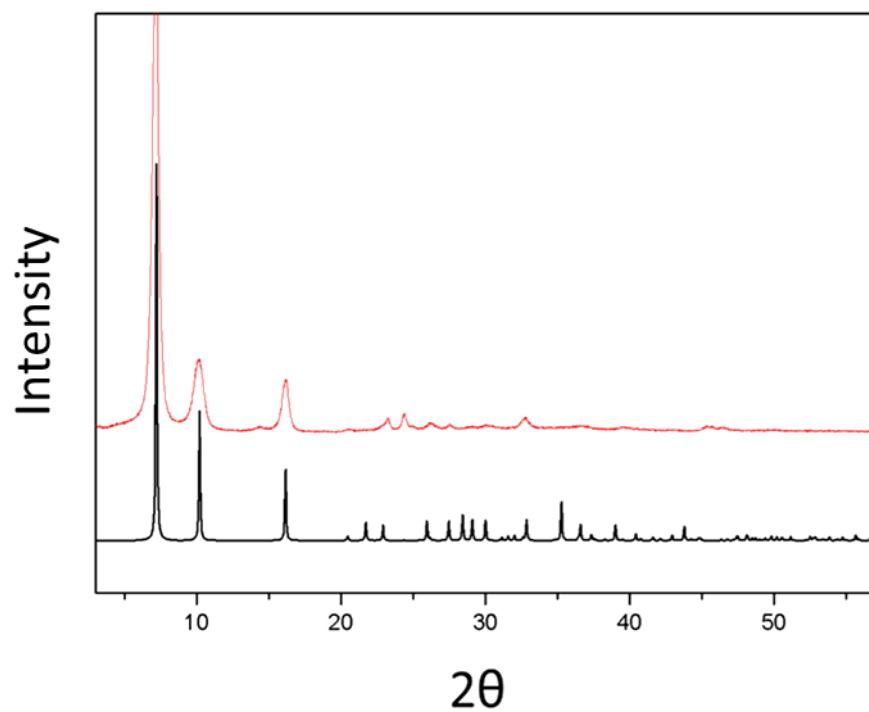


**Fig. S9.** Experimental (red) and simulated (black) XRPD patterns of  $[\text{Cu}(\text{TP})]_n$  (**2**).